International Journal of Pharmacy and Pharmaceutical Sciences

ISSN- 0975-1491 Vol 8, Issue 7, 2016

Original Article

IDENTIFICATION OF LEAD COMPOUNDS WITH COBRA VENOM DETOXIFICATION ACTIVITY IN *ANDROGRAPHIS PANICULATA* (BURM. F.) NEES THROUGH *IN SILICO* METHOD

N. C. NISHA, S. SREEKUMAR*, C. K. BIJU

Bioinformatics Centre, Saraswathy Thangavelu Centre, Jawaharlal Nehru Tropical Botanic Garden and Research Institute, Puthenthope, Thiruvananthapuram 695586, Kerala, India
***Email: drsreekumar@rediffmail.com**

Received: 12 Mar 2016 Revised and Accepted: 17 May 2016

ABSTRACT

Objective: To validate the cobra venom detoxification activity in *Andrographis paniculata* and identification of lead molecules.

Methods: The structures of phytochemicals were procured from databases or created by ChemSketch and CORINA. Of the14 cobra venom proteins selected as receptor molecules, the 3D structures of phospholipase A_2 and cobrotoxin were retrieved from protein data bank and serine protease, L-amino acid oxidase and acetylcholinesterase were modelled. The structures of remaining nine proteins were retrieved from SWISSMODEL repository. The active sites of the receptor molecules were detected by Q-site Finder and Pocket Finder. Docking was carried out by AutoDock 4.2. To avoid error in lead identification, top ranked five hit molecules obtained in AutoDock were again docked by iGEMDOCK, FireDock and HEX server. The results were analyzed following Dempster-Shafer theory. The molecular property and biological activity of the lead molecules were predicted by molinspiration.

Results: Docking results in AutoDock revealed that the plant having phytochemicals for detoxifying all venom proteins but only one potential hit molecule against each of the following proteins *viz*., cobramin A, cobramin B, long neurotoxin 1, long neurotoxin 2, long neurotoxin 3, long neurotoxin 4 and long neurotoxin 5 and several hit molecules (6-12) were obtained against phospholipase A_2, cobrotoxin, cytotoxin 3, acetylcholinesterase, L-aminoacid oxidase, proteolase and serine protease. Therefore, in latter case lead molecules were identified through Dempster-Shafer theory. The theoretical prediction of drug likeliness and bioactivity of the molecules highlighted the plant as the best source of anti-cobra venom drug.

Conclusion: The results substantiated its traditional use and further investigation on biological system is essential for evolving novel drug.

Keywords: *Andrographis paniculata*, Cobra, Docking, Venom, Protein, Neurotoxin, Snake bite

INTRODUCTION

The morbidity and mortality caused by snake bite especially in tropical countries like India are ten times greater than the infectious tropical neglected diseases identified by World Health Organization (WHO). Therefore, in 2009 WHO had included snake bite along with "Neglected Tropical Disease" [1]. The majority of the snake bite victims depend on traditional healers and their' details have not been documented. However, based on the available hospital records the annual death rate due to snake venom was estimated as 5.4-5.5 million globally and 20,000-1,25,000 in India [2]. Of the 60 venomous snake [3-4] species reported in India, four of them are common throughout India. Cobra (*Naja naja* L.) is one among them which causes a high rate of morbidity and mortality and its reasons have been well discussed [5]. Cobra venom is a complex mixture of bioactive molecules such as enzymes and other toxic proteins, lipids, carbohydrates, peptides, heavy metals, etc. More than 60 different molecules were isolated from the snake venom and many of them are used as drugs (Captopril, Enalapril, etc.) [6]. About 90 percent dry weight of venom constitutes proteins [7].

Formulating a single medicine against a mixture of toxic venom proteins is a herculean task. Antivenom therapy is the only treatment in modern medicine and it may induce several serious side effects to the patients. Its availability, storage facility, specificity, etc. in rural areas are also limiting factors. In these circumstances, most of the people depend on traditional herbal medicines which contain a plethora of chemical compounds and that can effectively neutralize the venom toxicity. Though 80% of the people depend on herbal medicines, its efficacy and molecular mechanism of drug action are seldom validated. The perusal of literature indicates that the plant *Andrographis paniculata* (Burm. F.) Nees has been used traditionally against snake venom particularly to treat cobra bite. The present investigation aimed to validate the cobra venom detoxification activity in *A. paniculata* and identification of potential lead molecules against each toxic protein.

MATERIALS AND METHODS

Preparation of macromolecules

Fourteen cobra (*Naja naja* L.) venom toxic proteins *viz*., phospholipase A_2, long neurotoxin 1, long neurotoxin 2, long neurotoxin 3, long neurotoxin 4, long neurotoxin 5, acetylcholinesterase, L-aminoacid oxidase, cobramin A, cobramin B, cytotoxin 3, cobrotoxin, serine protease and proteolase were selected as the receptor molecules for docking. The three-dimensional (3D) structures of phospholipase A_2 (1A3D) and cobrotoxin (1COD) were downloaded from RCSB Protein Data Bank. The modelled structures of the proteins such as cobramin A (Swiss-prot ID P01447), cobramin B (Swiss-prot ID P01440), cytotoxin 3 (Swiss-prot ID P24780), long neurotoxin 1 (Swiss-prot ID P25668), long neurotoxin 2 (Swiss-prot ID P25669), long neurotoxin 3 (Swiss-prot ID P25671), long neurotoxin 4 (Swiss-prot ID P25672), long neurotoxin 5 (Swiss-prot ID P25673) and proteolase (Swiss-prot ID Q9PVK7) were retrieved from SWISSMODEL repository. The 3D structure of serine protease was created using SWISSMODEL [8]. The primary sequence of serine protease of *N. naja* was retrieved from Swiss-prot (P86545) and submitted in BLASTp sequence similarity search tool. The template 1BQY_A was taken with 80% similarity and the protein was modelled.

The primary sequence data of L-aminoacid oxidase and acetylcholinesterase of *N. naja* were not available in protein databases. However, the sequence data of L-aminoacid oxidase from *Naja naja atra* (Chinese cobra) (Swiss-prot ID A8QL58) and acetylcholinesterase from *Naja naja oxiana* (Central Asian cobra) (Swiss-prot ID Q7LZG1), a close relative of *N. naja* were available in Swiss-prot database. Hence using these sequences, the templates such as 1EA5 for acetylcholinesterase and 1REO for L-aminoacid

oxidase were selected and 3D structures were created as reported earlier [9]. The active sites of all protein molecules were detected using the tools Q-site Finder and Pocket Finder.

Preparation of ligands

The literature survey and search on open access chemical databases revealed that about 109 chemical molecules were reported from *A. paniculata*. However, canonical SMILES of only 39 molecules were available on databases and the remaining 70 were drawn and its canonical SMILES were created using ChemSketch. The 3D structures of all molecules were created using CORINA. The molecules selected for docking were depicted in table 1.

Molecular docking

AutoDock 4.2

All selected phytochemicals were docked into the binding site of each of the fourteen cobra venom protein using AutoDock 4.2 following the procedure described by Morris *et al.* [9].

Table 1: List of selected phytochemicals in *Andrographis paniculata* for docking

S. No.	Compound and molecular formula	S. No.	Compound and molecular formula
1	(-)-3-ß-hydroxy 5-stigmata-9(11),22(23)-diene*,$C_{29}H_{48}O$	56	5-hydroxy-7,8-dimethoxy flavanone*, $C_{17}H_{16}O_5$
2	1,2-dihydroxy-6,8-dimethoxy xanthone*, $C_{15}H_{12}O_6$	57	5-hydroxy-7,8,2',6'-tetramethoxy flavone, $C_{19}H_{18}O_7$
3	1,8-dihydroxy-3,7-dimethoxy xanthone*, $C_{15}H_{12}O_6$	58	6'-acetyl neoandrographolide*, $C_{27}H_{40}O_9$
4	13,14,15,16-tetranorent labda-8(17)-ene-3,12,19-triol*, $C_{16}H_{28}O_3$	59	7,8,2'-trimethoxy flavone-5-ß-D-glucopyranosyloxy flavone*, $C_{24}H_{26}O_{11}$
5	14-acetyl 13,19-isopropylidene andrographolide*, $C_{25}H_{36}O_6$	60	7,8-dimethoxy flavone-5-ß-D-glucopyranosyloxy flavone*, $C_{23}H_{24}O_{10}$
6	14-acetyl andrographolide*, $C_{22}H_{32}O_6$	61	7-o-methyl wogonin*, $C_{17}H_{14}O_5$
7	14-α--lipoyl andrographolide*, $C_{28}H_{42}O_6S_2$	62	α-sitosterol, $C_{30}H_{50}O$
8	14-deoxy 11,12-didehydroandrographolide*, $C_{26}H_{38}O_9$	63	Andrograpanin, $C_{20}H_{30}O_3$
9	14-deoxy 11-oxo-andrographolide*, $C_{20}H_{28}O_4$	64	Andrograpanolide, $C_{21}H_{34}O_5$
10	14-deoxy 12-hydroxy andrographolide, $C_{20}H_{32}O_4$	65	Andrographidin A, $C_{23}H_{26}O_{10}$
11	14-deoxy 12-hydroxy andrographolide*, $C_{20}H_{30}O_5$	66	Andrographidin B, $C_{23}H_{24}O_{12}$
12	14-deoxy 14,15-didehydroandrographolide*, $C_{20}H_{30}O_4$	67	Andrographidin C, $C_{23}H_{24}O_{10}$
13	14-deoxy-11-hydroxyandrographolide, $C_{20}H_{30}O_6$	68	Andrographidin D, $C_{25}H_{28}O_{12}$
14	14-deoxy-12-methoxy andrographolide*, $C_{21}H_{32}O_5$	69	Andrographidin E, $C_{24}H_{26}O_{11}$
15	14-deoxy-15-isopropylidene-11,12-didehydroandrographolide*, $C_{23}H_{32}O_4$	70	Andrographidin F, $C_{25}H_{28}O_{13}$
16	14-deoxyandrographolide*, $C_{19}H_{28}O_5$	71	Andrographin, $C_{18}H_{16}O_6$
17	14-epiandrographolide, $C_{21}H_{32}O_5$	72	Andrographiside*, $C_{26}H_{40}O_{10}$
18	19-hydroxy-3-oxoentlabda-8(17),11,13-trien-16,15-olide*, $C_{20}H_{26}O_4$	73	Andrographolide, $C_{20}H_{30}O_5$
19	19-o-acetyl anhydroandrographolide*, $C_{22}H_{32}O_5$	74	Andrographoneo*, $C_{25}H_{38}O_{10}$
20	1-hydroxy-3,7,8-trimethoxy xanthone*, $C_{16}H_{14}O_6$	75	Andrographoside, $C_{26}H_{40}O_{10}$
21	2-(2'-benzyloxy)benzoyloxy-3,4,6-trimethoxy acetophenon*, $C_{25}H_{24}O_7$	76	Apigenin-7,4'-di-o-methyl ether*, $C_{17}H_{14}O_5$
22	2',5-dihydroxy-7,8-dimethoxy flavone-2'-O-ß-D-glucopyranoside*, $C_{23}H_{24}O_{11}$	77	Apigenin or 5,7,4'-trihydroxy flavone*, $C_{15}H_{10}O_6$
23	2-hydroxy-3,4,6,2'-tetramethoxy benzoylmethane*, $C_{19}H_{20}N_7$	78	ß-daucosterol*, $C_{35}H_{60}O_6$
24	2-hydroxy-5,7,8-trimethoxy flavone*, $C_{18}H_{16}O_6$	79	ß-sitosterol glucoside, $C_{35}H_{60}O_6$
25	3,14-dideoxyandrographolide*, $C_{20}H_{30}O_3$	80	Bisandrographolide ether*, $C_{46}H_{68}O_{13}$
26	3,15,19-trihydroxy ent labda-8(17),13-dien-16-oic acid*, $C_{20}H_{32}O_5$	81	Bisandrographolide A, $C_{40}H_{58}O_8$
27	3,18,19-trihydroxyentlabda-8(17),12-dien-16,15-olide*, $C_{20}H_{30}O_5$	82	Bisandrographolide B, $C_{40}H_{56}O_8$
28	3,19-dihydroxy-14,15,16-trinorentlabda-8(17),11-dien-13-oic acid*, $C_{17}H_{26}O_4$	83	Bisandrographolide C, $C_{40}H_{56}O_8$
29	3,19-dihydroxyentlabda-8(17),12-dien-16,15-olide*, $C_{20}H_{32}O_5$	84	Caffeic acid, $C_9H_8O_4$
30	3,19-isopropylidene andrographolide*, $C_{23}H_{34}O_5$	85	Carvacrol, $C_{10}H_{14}O$
31	3',2',5,7-tetramethoxy flavone*, $C_{17}H_{14}O_6$	86	Chlorogenic acid, $C_{16}H_{18}O_9$
32	3,4-dicaffeoyl quinic acid*, $C_{25}H_{24}O_{12}$	87	Cinnamic acid, $C_9H_8O_2$
33	3,7,8-trimethoxy 1-hydroxyxanthone*, $C_{16}H_{14}O_6$	88	Deoxyandrographiside*, $C_{26}H_{40}O_9$
34	3,7,8,2'-tetramethoxy 5-hydroxy flavone, $C_{19}H_{20}O_6$	89	Deoxyandrographolide, $C_{20}H_{30}O_4$
35	4,8-dihydroxy-2,7-dimethoxy xanthone*, $C_{15}H_{12}O_6$	90	Dicaffeol acid*, $C_{31}H_{64}$
36	4-hydroxy-2-methoxy cinnamaldehyde*, $C_{10}H_{10}O_3$	91	Ent-14-ß-hydroxy-8(17),12-laba diene-16,15-olide-3-ß-19-oxide*, $C_{20}H_{28}O_4$
37	4'-hydroxy-7,8,2',3'-tetramethoxy flavone-5-ß-D-glucopyranosyloxy flavone*, $C_{24}H_{26}O_{13}$	92	Ent-labda-8(17),13-diene-15,16,19-triol*, $C_{20}H_{32}O_3$
38	5,2',6'-trihydroxy-7-methoxy flavone 2'-O-ß-D-glucopyranoside*, $C_{22}H_{22}O_{11}$	93	Ergosterol peroxide, $C_{28}H_{44}O_3$
39	5,2'-dihydroxy-7,8,-dimethoxy flavone-3'-ß-D-glucopyranosyloxy flavone*, $C_{22}H_{22}O_{12}$	94	Eugenol, $C_{10}H_{12}O_2$
40	5,2'-dihydroxy-7,8-dimethoxy flavone or skullcapflavone, $C_{18}H_{16}O_6$	95	Hentriacontane, $C_{31}H_{64}$
41	5,3'-dihydroxy-7,8,4'-trimethoxy flavone*, $C_{18}H_{16}O_7$	96	Myristic acid, $C_{14}H_{28}O_2$
42	5,4'-dihydroxy-7,8,2',3'-tetramethoxy flavone, $C_{19}H_{18}O_8$	97	Neoandrographolide*, $C_{26}H_{40}O_8$
43	5,5'-dihydroxy-7,8,2'-trimethoxy flavone*, $C_{18}H_{16}O_7$	98	Oleanolic acid, $C_{30}H_{48}O_3$
44	5,7,2',3'-tetramethoxy flavanone*, $C_{19}H_{20}O_6$	99	Onysylin*, $C_{17}H_{16}O_5$
45	5,7,8,2'-tetramethoxy flavone*, $C_{19}H_{18}O_6$	100	Oroxylin A*, $C_{16}H_{12}O$
46	5,7,8-trimethoxy-2'-hydroxy flavone*, $C_{18}H_{16}O_3$	101	Panicolin, $C_{17}H_{14}O_6$

47	5,7,3',4'-tetrahydroxy flavone, $C_{15}H_{12}O_6$	102	Paniculide A*, $C_{15}H_{22}O_4$
48	5-hydroxy-7,2',6'-trimethoxy flavone*, $C_{18}H_{16}O_6$	103	Paniculide B*, $C_{15}H_{20}O_5$
49	5-hydroxy-7,8,2',3'-tetramethoxy flavone *, $C_{19}H_{18}O_7$	104	Paniculoside I, $C_{26}H_{40}O_8$
50	5-hydroxy-7,8,2',3',4'-pentamethoxy flavone*, $C_{20}H_{20}O_8$	105	Quinic acid, $C_7H_{12}O_6$
51	5-hydroxy-7,8,2',5'-tetramethoxy flavone*, $C_{19}H_{18}O_7$	106	Stigmasterol, $C_{29}H_{48}O$
52	5-hydroxy-7,8,2'-trimethoxy flavone*, $C_{18}H_{16}O_6$	107	Tritricontane, $C_{33}H_{68}$
53	5-hydroxy-2'-ß-D-glucosiloxy-7-methoxy flavone*, $C_{22}H_{22}O_{10}$	108	Wightinolide*, $C_{20}H_{32}O_4$
54	5-hydroxy-3,7,8,2'-tetramethoxy flavanone, $C_{19}H_{20}O_6$	109	Wogonin*, $C_{16}H_{12}O_5$
55	5-hydroxy-7,2',3'-trimethoxy flavone*, $C_{18}H_{16}O_6$		

*Drawn by ChemSketch

Table 2: Lead identification following Dempster-Shafer theory analysis

Hit molecules	Venom proteins	Docking score (DST class)				Rank sum
		AutoDock	iGEMDOCK	Fire dock	Hex server	
Andrographin	Phospholipase A_2	-8.47 (1)	-92.8065 (1)	-48.84 (1)	-234.84 (1)	4
5,2'-dihydroxy-7,8-dimethoxy flavone-3'-ß-D-glucopyranosyloxy flavone		-8.45 (1)	-113.03 (4)	-46.16 (1)	-295.52 (4)	10
19-O-acetyl an hydro andrographolide		-8.78 (4)	-88.2897 (1)	-51.4 (2)	-227.53 (1)	8
5-hydroxy-2'-ß-D-glucosiloxy-7-methoxy flavone		-8.81 (4)	-114.223 (4)	-59.93 (4)	-287.33 (4)	16
19-hydroxy-3-oxoentlabda-8(17),11,13-trien-16,15-olide	Acetylcholinesterase	-6.78 (1)	-85.138 (4)	-38.67 (2)	-215.82 (2)	9
Andrograpanin		-6.41 (1)	-65.2686 (1)	-36.57 (1)	-224.15 (3)	6
Ent-14-ß-hydrox y-8(17),12-labadiene-16,15-olide-3-ß-19-oxide		-7.63 (4)	-75.925 (3)	-42.74 (4)	-200.23 (1)	12
Stigmasterol		-7.96 (4)	-76.9134 (3)	-41.5 (4)	-243.65 (4)	15
Bisandrographolide A	L-aminoacid oxidase	-10.18 (4)	-103.804 (4)	-53.75 (4)	-383.54 (4)	16
Bisandrographolide B		-9.38 (2)	-105.588 (4)	-50.56 (3)	-373.67 (4)	13
Bisandrographolide C		-9.06 (1)	-98.9506 (2)	-46.64 (1)	-350.78 (2)	6
Ergosterol peroxide		-9.72(3)	-94.555 (1)	-52.35 (4)	-329.4 (1)	9
Andrograpanin	Cytotoxin 3	-5.64 (4)	-74.9573 (4)	-22.74 (1)	-12.36 (2)	11
3,14-dideoxyandrographolide		-5.46 (1)	-69.8947 (1)	-22.98 (1)	-13.65 (4)	8
Deoxy andrographolide		-5.5 (2)	-64.848 (2)	-26.91 (3)	-12.98 (3)	9
Ent labda-8(17),13-diene-15,16,19-triol		-5.4 (3)	-70.5113 (1)	-30.1 (4)	-11.2 (1)	9
3,15,19-trihydroxy entlabda-8(17),13-dien-16-oic acid	Cobrotoxin	-11.2 (4)	-117.732 (3)	-32.61 (1)	-230.65 (1)	9
19-hydroxy-3-oxoentlabda-8(17),11,13-trien-16,15-olide		-9.45 (1)	-124.484 (4)	-53.68 (4)	-226.06 (1)	10
Ent-14-ß-hydroxy-8(17),12-labadiene-16,15-olide-3-ß-19-oxide		-9.88 (1)	-107.993 (1)	-35.13 (1)	-223.93 (1)	4
Oleanolic acid		-10.58 (3)	-106.886 (1)	-34.06 (1)	-251.91 (4)	9
3,19-dihydroxy-14,15,16-trinorentlabda-8(17),11-dien-13-oic acid	Serine protease	-5.44 (2)	-79.8456 (3)	-48.52 (4)	-217.69 (2)	11
13,14,15,16-tetranorentlabd-8(17)ene-3,12,19-triol		-5.57 (4)	-78.5654 (2)	-45.5 (1)	-207.51 (1)	8
Apigenin-5,7,4'-trihydroxy flavone		-5.34 (1)	-83.1209 (4)	-44.85 (1)	-207.74 (1)	7
Apigenin-7,4'-dimethyl ether		-5.39 (1)	-76.1197 (1)	-45.14 (1)	-234.34 (4)	7
3,19-isopropylidene andrographolide	Proteolase	-7.17 (2)	81.3341 (1)	-52.8 (4)	-269.5 (3)	10
7,8-dimethoxy flavone-5-ß-D-glucopyranosyloxy flavone		-7.05 (1)	-104.478 (4)	-49.83 (2)	-292.11 (4)	11
14-acetyl-3,19-isopropylidene andrographolide		-7.33 (4)	-82.6491 (1)	-46.97 (1)	-282.97 (4)	10
14-deoxy-14,15-didehydro andrographolide		-7.12 (2)	-83.9643 (1)	-48.42 (1)	-244.68 (1)	5

Active residues of phospholipase A_2, cobramin A, cobramin B, cytotoxin 3 and proteolase were available in Uni Prot database and the same residues were used for docking. The active sites of the remaining proteins were detected using the software applications Pocket-Finder and Q-Site Finder.

The grid spacing and selection of all parameters for docking and analysis of docked results were done as reported earlier [5]. The top-ranked molecules with the free energy of binding ≤-5 kcal/mol were considered as hit molecules, and these molecules were further analyzed by Lipinski's rule of five and rule of three for drug-likeness characters such as Absorption, Distribution, Metabolism and Excretion (ADME). To reduce error during lead selection, the first four top ranked hits in AutoDock were further docked with other docking tools such as iGEMDOCK [10], FireDock (http://bioinfo3d.cs.tau.ac.il/FireDock/) [11] and HEX server [12]. The scores obtained were statistically analyzed following Dempster-Shafer theory (DST) and potential lead molecules were recognized.

Post data analysis

The docked results in AutoDock 4.2, iGEMDOCK, FireDock and HEX server were documented in axls spreadsheet file format and uploaded on the website http://allamapparao.org/dst/application tool. The uploaded data were parsed and stored in 2D array and subsequently analyzed as follows 1) divide the data into four classes; 2) get a result from Rank Sum Technique; 3) get a result from DST unweight; 4) get results from DST weighted; 5) get results from Zhang Rule. The top-ranked molecules obtained from the 2-5 procedures [13] were selected as lead molecules and considered for further investigations.

Drug likeliness prediction

Molinspiration property prediction tool

To analyze the drug-likeness of the hit molecules for its property prediction, each molecule was submitted on open access molinspiration property prediction tool (www.molinspiration. com). The tool analyzes the molecular properties based on Lipinski's rule of five and violation in the particular property will be provided. The software was used to calculate MiLogP, total polar surface area (TPSA) and drug likeness. MiLogP (Octanol/water partition coefficient) is the parameter used to predict the permeability of the molecule across the cell membrane and calculated through the methodology developed by molinspiration, as a sum of fragment-based contributions and correction factors.

This tool analyzes the molecular properties such as miLogP, TPSA, MW, ON, OHNH, ROTB and Volume from the three-dimensional structure of the given molecule. The miLogP was obtained by fitting calculated logP with experimental logP for a training set of drug like molecules which describes the oral activity of a molecule. TPSA is used to predict the drug absorption, including intestinal absorption, bioavailability, Caco-2 permeability and blood-barrier penetration. TPSA is calculated through the sum of fragment-based contributions of O-and N-centered polar fragments and the surface areas occupied by hydrogen bound oxygen and nitrogen atoms.

The nrotb (number of rotatable bonds) is a topological parameter which defines the measures of molecular flexibility and a good parameter for oral bioavailability [14]. Molecular volume determines transport of molecules such as blood-barrier penetration and intestinal absorption [15].

Biological activity prediction

Each biologically active compound possesses a number of biological activities. The bioactivity score of each lead molecule was calculated for GPCR ligand, ion channel modulator, kinase inhibitor and nuclear receptor ligand with the help of molinspiration software.

RESULTS

Docking between 109 chemical molecules derived from *A. paniculata* and each of the fourteen cobra venom protein indicated that the plant has neutralizing activity on all toxic venom proteins. The docking scores obtained in AutoDock 4.2 showed that to neutralize the activity of each of the following protein *viz*., cobramine A, cobramine B, long neurotoxin 1, long neurotoxin 2, long neurotoxin 3, long neurotoxin 4 and long neurotoxin 5 only one hit molecule and for others several hit molecules were present. Hit molecules identified against the former were quinic acid on cobramin A, cinnamic acid on cobramin B, α-sitosterol on long neurotoxin 1 and 4-hydroxy-2-methoxy cinnamaldehyde on the remaining long neurotoxins.

Several hit molecules (6-102) were obtained from the proteins such as phospholipase A_2 (77), acetylcholinesterase (54), L-aminoacid oxidase (21), cytotoxin 3 (6), cobrotoxin (102), proteolase (67) and a serine protease (12).

Hence, to avoid error in lead identification four top ranked hit molecules of each protein were further docked using three more tools such as iGEMDOCK, FireDock and HEX server and lead molecules were selected through DST (table 2).

The selected lead molecule on each protein such as 5-hydroxy-2'-ß-D-glucosiloxy-7-methoxy flavones on phospholipase A_2, 19-hydroxy-3-oxoentlabda-8(17),11,13-trien-16,15-olide on cobrotoxin, andrograpanin on cytotoxin 3, stigmasterol on acetylcholinesterase, bis andrographolide A on L-aminoacid oxidase, 7,8-dimethoxy flavone-5-ß-D-glucopyranosyloxy flavones on proteolase and 3,19-dihydroxy-14,15,16-trinorentlabda-8(17),11-dien-13-oic acid on serine protease were depicted in fig. 1.

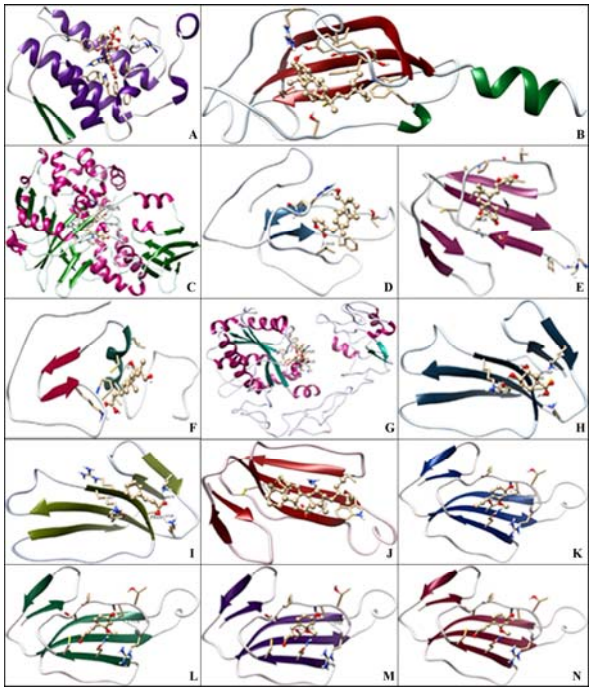

Fig. 1: Docked structures of venom proteins and lead molecules, A) Phospholipase A_2 and 5-hydroxy-2'-ß-D-glucosiloxy-7-methoxy flavone, B) Acetylcholinesterase and stigmasterol, C) L-aminoacid oxidase and bis andrographolide A, D) Cytotoxin3 and andrograpanin, E) Cobrotoxin and 19-hydroxy-3-oxoentlabda-8(17),11,13-trien-16,15-olide, F) Serine protease and 3,19-dihydroxy-14,15,16-trinorentlabda-8(17),11-dien-13-oic acid, G) Proteolase and 7,8-dimethoxy flavone-5-ß-D-glucopyranosyloxy flavones, H) Cobramin A and quinic acid, I) Cobramin B and cinnamic acid, J) Long neurotoxin 1 and α-sitosterol, K) Long neurotoxin 2 and 4-hydroxy-2-methoxy cinnamaldehyde, L) Long neurotoxin 3 and 4-hydroxy-2-methoxy cinnamaldehyde, M) Long neurotoxin 4 and 4-hydroxy-2-methoxy cinnamaldehyde, N) Long neurotoxin 5 and 4-hydroxy-2-methoxy cinnamaldehyde

The molecular interaction between the docked structure in AutoDock as follows. Phospholipase A_2 and 5-hydroxy-2'-ß-D-glucosiloxy-7-methoxy flavone showed one hydrogen bond (GLY29: HN), bond type N-H. O and bond length 1.933Å. Acetylcholinesterase and stigmasterol showed only one H-bond (TYR63:H65), bond type O-H. O and bond length 2.175Å. Similarly, long neurotoxin 1 and α-sitosterol showed one H-bond (CYS41:HN), bond type N-H. O and bond length 1.911Å.

However, long neurotoxin 2 and 4-hydroxy-2-methoxy cinnamaldehyde possess two H-bonds (THR22:HG1 and GLN55:HE22), bond types O-H. O and N-H. O and bond lengths 2.039Å and 1.931Å respectively. Likewise, long neurotoxin 3, 4 and 5 showed two H-bonds with 4-hydroxy-2-methoxy cinnamaldehyde. They were PRO71:H18 and GLN55:HE22, THR22:HG1 and GLN55:HE22 and PRO71:H18 and GLN55:HE22, bond types O-H. O and N-H. O and bond lengths 1.7Å and 1.994Å, 1.983Å and 2.077Å and 1.872Å and 1.903Å respectively.

Cobramine A and quinic acid showed four H-bonds (LYS12: HZ1 1, CYS38:HN 1, TYR22:H25 1 and TYR22:H24 1), bond types N-H. O, N-H. O, O-H. O and O-H. O and bond length 2.138Å, 1.934Å, 2.145Å and 2.092Å respectively. Cobramine B and cinnamic acid showed two H-bonds LYS12:HZ1 and LYS18:HZ2, bond type N-H. O and bond lengths 1.997Å and 1.973Å. L-amino acid oxidase and bis andrographolide A showed six H-bonds (THR447:H80, SER445:H98, ARG109:HE 0, ARG109:HH22, ARG339:HH21 and TYR389:HH) bond types O-H. O, O-H. O, N-H. O, N-H. O, N-H. O and O-H. O, bond lengths 1.921Å, 1.951Å, 2.248Å, 2.106Å, 1.889Å and 2.000Å respectively.

Cytotoxin 3 and andrograpanin showed two H-bonds (ASN60:H53 and VAL52:HN), bond types O-H. O and N-H. O and bond lengths 2.06Å and 2.238Å respectively. Cobrotoxin and 19-hydroxy-3-oxoentlabda-8(17),11,13-trien-16,15-olide showed one H-bond (GLY40:H), bond type N-H. O and bond length 1.940Å. Proteolase and 7,8-dimethoxy flavone-5-ß-D-glucopyranosyloxy flavones have no H-bonds. Finally, serine protease and 3,19-dihydroxy-14,15,16-trinorentlabda-8(17),11-dien-13-oic acid showed only one H-bond (LEU18:H41), bond type O. H-O and bond length 1.919Å. The analysis of H-bond interaction revealed that all the lead molecules possess strong H-bonds with the respective venom proteins since the bond types were N-H. O and O-H. O and bond length range from 1.7Å to 2.5Å. The drug likeliness of the lead molecules was analyzed through molinspiration property prediction tool (table 3).

Table 3: Prediction of drug likeliness properties of lead molecules by molinspiration

Lead molecule	MiLogP	TPSA	Atoms	MW	# ON	# OHNH	#Violations	#ROTB	Volume
19-hydroxy-3-oxoentlabda-8(17),11,13-trien-16,15-olide	1.373	63.604	24	330.424	4	1	0	3	318.239
3,19-dihydroxy-14,15,16-trinorentlabda-8(17),11-dien-13-oic acid	1.674	77.755	21	294.391	4	3	0	3	289.758
4-hydroxy-2-methoxy cinnamaldehyde	1.81	46.533	13	178.187	3	1	0	3	164.007
5-hydroxy-2'-ß-D-glucosiloxy-7-methoxy flavone	1.164	159.05	32	446.408	10	5	0	5	373.698
7,8-dimethoxy flavone-5-ß-D-glucopyranosyloxy flavone	1.266	148.06	33	460.435	10	4	0	6	391.226
α-sitosterol	8.151	20.228	31	426.729	1	1	1	5	466.891
Andrograpanin	2.873	46.533	23	318.457	3	1	0	4	322.244
Bisandrographolide A	4.611	133.52	48	666.896	8	4	1	9	647.993
Cinnamic acid	1.91	37.299	11	148.161	2	1	0	2	138.462
Quinic acid	-2.33	118.21	13	192.167	6	5	0	1	161.456
Stigmasterol	7.869	20.228	30	412.702	1	1	1	5	450.33

The bioactivity of the lead molecules as GPCR ligand, ion channel modulaor, kinase inhibitor, nuclear receptor ligand, protease inhibitor and enzyme inhibitory activity were predicted (table 4).

Table 4: Bioactivity score of the selected lead molecules

Lead molecules	GPCR ligand	Ion channel modulator	Kinase inhibitor	Nuclear receptor ligand	Protease inhibitor	Enzyme inhibitor
19-hydroxy-3-oxoentlabda-8(17),11,13-trien-16,15-olide	0.18	0.08	-0.33	0.75	-0.06	0.53
3,19-dihydroxy-14,15,16-trinorentlabda-8(17),11-dien-13-oic acid	0.27	0.14	-0.25	0.98	0.13	0.77
4-hydroxy-2-methoxy cinnamaldehyde	-0.69	-0.27	-0.78	-0.34	-0.62	-0.23
5-hydroxy-2'-ß-D-glucosiloxy-7-methoxy flavones	0.06	-0.05	0.1	0.25	-0.05	0.42
7,8-dimethoxy flavone-5-ß-D-glucopyranosyloxy flavones	-0.03	-0.04	0.02	-0.01	-0.12	0.30
α-sitosterol	0.15	0.15	-0.34	0.89	-0.13	0.66
Andrograpanin	0.43	0.11	-0.37	0.76	0.07	0.63
Bisandrographolide A	-0.22	-1.03	-0.95	-0.38	-0.15	-0.26
Cinnamic acid	-0.74	-0.40	-1.14	-0.47	-0.99	-0.30
Quinic acid	-0.24	0.1	-0.77	0.16	-0.26	0.60
Stigmasterol	0.12	-0.08	-0.49	0.74	-0.02	0.53

DISCUSSION

Andrographis paniculata is widely used as an antidote to snakebite in general and particularly against cobra venom [16]. The *in vitro* and *in vivo* experimental results showed the same effect [17-19]. However, identification of the molecules responsible for detoxification and its mode of the molecular mechanism of interaction with toxic venom proteins were seldom investigated. Cobra venom is a mixture of fourteen toxic proteins. Of these, lion share is phospholipase A_2, which is the main cause of lethality.

Others mainly cause serious lifelong morbidity to the victims and therefore, detoxification of all venom proteins is inevitable. Docking between each of the venom protein of a particular snake species and all phytochemicals from the desired plant species is the best option to identify the potential lead molecules against each venom toxic protein [5]. Among the docking tools, AutoDock is a widely used and reliable one. Out of 109 phytochemicals screened against 14 venom proteins using the tool AutoDock, several phytochemicals with minimum binding energy level differences were noticed against seven proteins. Therefore, in order to avoid error in lead selection, such molecules were again docked using four different tools, and the results were statistically analyzed following DST method for the identification of lead molecules.

The molecular interaction between lead molecules with toxic venom proteins showed that most of the lead molecules have strong hydrogen bond at the active residues of the venom proteins. Theoretically, a drug-like molecule has logP range of-0.4 to 5.6, molecular weight 160-480 g/mol, molar refractivity of 40-130 (related to the volume and molecular weight), 20-70 atoms and follow other Lipinski's rule of five [20]. After the prediction of molecular properties, the tool compared it with Lipinski's rule of five and found that among the selected lead molecules only three of them showed violation in a single property, i.e., α-sitosterol and stigmasterol showed violation in MiLogP and the values are 8.151 and 7.869 respectively. The molecule bis andrographolide A showed violation in its molecular weight (666.89 g/mol). Generally, natural compounds violate Lipinski's rule of five [21].

Generally, the higher value of bioactivity score is directly proportional to the activity of a molecule as a drug. The molecule possesses bioactivity score higher than 0.00 can be considered as a higher possibility of biological activity. The score between-0.50 to 0.00 shows moderate and the value less than-0.50 may be inactive. The results of bioactivity score of the selected molecules (table 4) showed that all the molecules possess potential activity as enzyme inhibitor and nuclear receptor ligand. Also, the molecules showed high score in all other bioactivity parameters. The 4-hydroxy-2-methoxy cinnamaldehyde and cinnamic acid violate protease inhibitor activity (-0.62 and-0.99) and GPCR ligand (-0.69 and-0.74). Similarly, 4-hydroxy-2-methoxy cinnamaldehyde, bisandrographolide A, cinnamic acid and quinic acid violate kinase inhibitor activity (-0.78,-1.14 and-0.77). The high bioactivity score of lead molecules predicts their potential activity in *in vivo*. The overall results confirmed the traditional knowledge as antidote snake activity in *A. paniculata*.

CONCLUSION

The overall results revealed that *A. paniculata* contains phytoactive molecules which can effectively neutralize all the fourteen toxic cobra venom proteins. The theoretical prediction of drug-likeness and bioactivity of the lead molecules ensured the potentiality of the lead molecules as a drug. However, theoretical prediction of drug likeliness only gives probability and its activity in a biological system is essential. Although, preliminary *in vitro* and *in vivo* tests were reported further in-depth experiments in this line is necessary for developing the lead molecules as a drug.

ACKNOWLEDGEMENT

We thank Department of Science and Technology, Govt. of India, New Delhi for financial support, the Director, JNTBGRI and Dr. T. Madhan Mohan, Advisor, DBT for providing the facilities and encouragements.

CONFLICT OF INTERESTS

Declared none

REFERENCES

1. Mukherjee AK. Green medicine as a harmonizing tool to antivenom therapy for the clinical management of snakebite: the road ahead. Indian J Med Res 2012;136:10-2.
2. Williams D, Gitierrez JM, Harrison R, Warrel DA, White J, Winkel KD, *et al.* The global snakebite initiative: an antidote for snake bite. Lancet 2010;375:89-91.
3. Narvencar K. Correlation between the timing of ASV administration and complications in snake bites. J Assoc Physicians India 2006;54:717-9.
4. Gupta YK, Peshin SS. Snake bite in India: the current scenario of an old problem. J Clin Toxicol 2014;4:43-9.
5. Nisha NC, Sreekumar S, Biju CK, Krishnan PN. Identification of lead compounds with cobra venom neutralizing activity in three Indian medicinal plants. Int J Pharm Pharm Sci 2014;6:536-41.
6. Nisha NC, Sreekumar S, Biju CK, Krishnan PN. Snake anti-venom: virtual screening of plant-derived molecules. Biobytes 2010;6:14-22.
7. Lalla JK, Sunita Ogale, Priyanka Goswami, Zaid Temrikar, Geeta Talele. Snake bite problem in India: an overview. Sch Acad J Pharm 2013;2:252-9.
8. Peitsch MC. Protein modeling. Bio/Technol Nat Biotechnol 1995;13:658-60.
9. Morris GM, Huey R, Lindstrom W, Sanner MF, Belew RK, Goodsell DS, *et al.* "AutoDock4 and AutoDock Tools4: Automated docking with selective receptor flexibility. J Comput Chem 2009;30:2785-91.
10. Hsu KC, Chen YF, Lin SR, Yang JM. iGEMDOCK: A graphical environment of enhancing GEMDOCK using pharmacological interactions and post-screening analysis. BMC Bioinformatics 2011;12(Suppl 1)S33.
11. http://bioinfo3d.cs.tau.ac.il/FireDock. [Last accessed on 10 Feb 2016].
12. Macindoe G, Mavridis L, Venkatraman V. Hex server: an FFT-based protein docking server powered by graphics processors. Nucleic Acids Res 2010;38:445-9.
13. Rao GN, Rao AA, Rao PS, Muppualaneni NB. A tool for the post data analysis of screened compounds derived from computer-aided docking scores. Bioinformation 2013;9:207-9.
14. Verma A. Lead finding from *Phyllanthus debelis* with hepatoprotective potentials. Asian Pac J Trop Biomed 2012;2:1735-7.
15. Lalitha P, Sivakamasundari S. Calculation of molecular lipophilicity and drug likeness for few heterocycles. Orient J Chem 2010;26:135-41.
16. Kulyal P, Tiwari UK, Shukla A, Gaur AK. Chemical constituents isolated from *Andrographis paniculata*. Indian J Chem 2010;49:356-9.
17. Gopi K, Renu K, Raj M, Kumar D, Muthuvelan B. The neutralization effect of methanol extract of *Andrographis paniculata* on Indian cobra *Naja naja* snake venom. J Pharm Res 2011;4:1010-2.
18. Premendran SJ, Salwe KJ, Pathak S, Brahmane R, Manimekalai. Anticobra venom activity of plant *Andrographis paniculata* and its comparison with polyvalent anti-snake venom. J Nat Sci Biol Med 2011;2:198–204.
19. Meenatchisundaram S, Prajish, Parameswari G, Subbraj T, Michael A. Studies on antivenom activity of *Andrographis paniculata* and *Aristolochia indica* plant extracts against *Echis carinatus* venom. Internet J Toxicol 2009;6:1.
20. Ghose AK, Viswanadhan VN, Wendoloski JJ. A knowledge-based approach in designing combinatorial or medicinal chemistry libraries for drug discovery. J Comb Chem 1999;1:55–68.
21. Ganesan A. The impact of natural products upon modern drug discovery. Curr Opin Chem Biol 2008;12:306-7.